MicroRNA-376b-3p ameliorates nonalcoholic fatty liver disease by targeting FGFR1 and regulating lipid oxidation in hepatocytes

Xin-Yu Wang[1], Lin-Jie Lu[1], You-Ming Li[1], Cheng-Fu Xu[1,*]

[1] Department of Gastroenterology, the First Affiliated Hospital, Zhejiang University School of Medicine, Hangzhou 310003, China

[*] **Corresponding author:**

Cheng-Fu Xu, M.D.

Department of Gastroenterology, the First Affiliated Hospital, Zhejiang University School of Medicine, 79 Qingchun Road, Hangzhou 310003, China.

Telephone: +86-571-87236863

E-mail: xiaofu@zju.edu.cn

Abstract

Background and aims: Nonalcoholic fatty liver disease (NAFLD) is a common chronic liver disease, whose molecular mechanisms remain unclear. This study aimed to explore the role and mechanisms of microRNA-376b-3p in NAFLD.

Methods: We analyzed the miRNA expression profiles of NAFLD by microarray and validated the expression of microRNA-376b-3p in cellular and mouse models of NAFLD. We also explored the role and downstream mechanisms of microRNA-376b-3p in NAFLD.

Results: Microarray analysis and subsequent validation showed that miR-376b-3p was markedly down-regulated in the livers of HFD-fed mice and in FFA-stimulated hepatocytes. MiR-376b-3p supplementation ameliorated hepatic steatosis and miR-376b-3p inhibition aggravates hepatic lipid accumulation both in vivo and in vitro. Luciferase report assay indicated that Fgfr1 is the direct target gene of miR-376b-3p and miR-376b-3p regulates fatty acids oxidation by targeting Fgfr1 to influence the development of NAFLD.

Conclusions: MiR-376b-3p was downregulated in NAFLD and has a novel regulatory role in lipid oxidation through miR-376b-3p-Fgfr1 dependent mechanism.

Key words: miR-376b-3p; NAFLD; Fgfr1; Lipid oxidation

1. Introduction

Nonalcoholic fatty liver disease (NAFLD) refers to a clinicopathological syndrome characterized by excessive hepatic lipid accumulation without excess alcohol intake and other definite liver damage factors[1]. It is now the most common clinical chronic liver disease worldwide, ranging from simple steatosis to steatohepatitis, fibrosis, cirrhosis, and eventually hepatic carcinoma[2, 3]. NAFLD is also closely related to the high incidence of metabolic syndrome, coronary heart disease, type 2 diabetes, chronic kidney disease, and extrahepatic malignancie[4]. Although, intensive investigations have been carried out during past decades, the pathogenesis of NAFLD remains largely unknown.

MicroRNA (miRNA) is a class of endogenous non-coding small RNA molecules that can regulate biological processes by changing the expression and translation of target gene messenger RNA (mRNA) at the post-transcriptional level[5]. A growing number of studies implicated that the expression and regulation of miRNAs are related to liver metabolic reprogramming and play an important role in NAFLD[6]. For instance, miR-122, which is the most abundant miRNA in human liver, could prevent hepatic steatosis by decreasing expression of lipogenic genes[7]. Previous study found that miR-34a was elevated in the haptic of HFD-fed mice, and induced hepatic lipid accumulation targeting to peroxisome proliferator-activated receptor α (PPARα)[8]. However, whether the effects of miRNA-376b-3p on hepatocytes lipid accumulation is remains unclear.

In this study, we analyzed the hepatic miRNA expression profiles of HFD-fed mice and found that miR-376b-3p is involved in the hepatocytes lipid accumulation via regulation of lipid oxidation by targeting fibroblast growth factor receptor 1 (FGFR1).

2. Materials and Methods

2.1. Animal Treatment

Male C57BL/6 mice (8-10 weeks old) were purchased from the Experimental Animal Centre of Zhejiang Province (Hangzhou, China). Mice were housed in an air-conditioned specific pathogen-free (SPF) conditions with a 12-hour light/dark cycle in a temperature-controlled environment (23 ±2°C), with *ad libitum* access to food and water. To establish an NAFLD model, mice were fed with a high fat diet (HFD, Research Diet, New Brunswick, NJ) for eight weeks, while control mice received standard chow diet (SCD). Western diet (WD, Research Diet, New Brunswick, NJ) was fed to mice for 24 weeks, while SCD fed to control mice. All mouse experimental procedures were approved by the Animal Care and Use Committee of the First Affiliated Hospital, Zhejiang University School of Medicine.

2.2. Cell cultures and treatments

Primary hepatocytes were isolated from 8-week-old mice after liver perfusions. The human hepatoblastoma cell line (HepG2) and mouse hepatocytes cell line (AML-12) were purchased from the Chinese Academy of Science (Shanghai, China). HepG2 cells were cultured in Dulbecco's modified eagle medium (DMEM) supplemented with 10% FBS and 1% penicillin/streptomycin. AML-12 cells were grown in Dulbecco's Modified Eagle Medium/Nutrient Mixture F-12 (DMEM/F12) with 10% FBS, 1% penicillin/streptomycin, and ITS Liquid Media Supplement (40μg/ml). Cells were incubated at 37 ^{o}C in a 5% CO_2 condition. Cells were exposed to 1mM FFA

mixture (2:1 ratio of oleate and palmitate, Sigma, Madrid, Spain) for 24 h to establish a NAFLD cellular model.

2.3. Cell transfection

Mmu/has-miR-376b-3p inhibitor, mmu/has-miR-376b-3p mimic, Fgfr1 siRNA, over-expression plasmids of Fgfr1, and their corresponding negative controls were purchased from RiboBio (Guangzhou, China). Cells were transfected with the miRNA inhibitor, miRNA mimic, siRNAs and plasmids via Lipofectamine3000 (Invitrogen, Carlsbad, CA) according to the manufacturer's instructions. 24h after transfection, the hepatocytes were exposed to FFA for another 24 h.

2.4. miRNA array

Total RNA was isolated and the RNA integrity was assessed using Agilent Bioanalyzer 2100 (Agilent Technologies, Santa Clara, CA). The total RNA was transcribed to double strand cDNA, then synthesized into cRNA and labeled with Cyanine-3-CTP. The labeled cRNAs were hybridized onto the microarray, and the arrays were scanned by the Agilent Scanner G2505C (Agilent Technologies). Feature Extraction software (version 10.7.1.1, Agilent Technologies) was used to analyze array images to get raw data. Genespring (version 14.8, Agilent Technologies) were employed for the basic analysis of the raw data. The raw data was normalized with the quantile algorithm. The threshold set for up- and down-regulated genes was a fold change $\geq$ 1.5.

104

105 **2.5. Tail vein injection of lentiviral vector**

106 Male C57BL/6 mice were acclimated for 1 week after arrival before they were used
107 for experiments. The sequence of miR-376b-3p mimic or inhibitor was built to
108 pLenti6.3/TO/V5 vector (Invitrogen, Carlsbad, USA). The mice were injected with 2
109 $\times 10^{11}$ TU/ml lentiviral vector or negative control vector via tail vein one week before
110 HFD or SCD treatment.

111

112 **2.6. Glucose tolerance test (GTT) and insulin tolerance test (ITT)**

113 For GTT, mice were fasted for 16 h followed by intraperitoneal injection of 1 g/kg of
114 glucose (Sigma–Aldrich). For ITT, mice were fasted for 6 h followed by
115 intraperitoneal injection of 0.75 U/kg of regular human insulin (Wanbang, Xuzhou,
116 China). Blood glucose was determined at 0, 15, 30, 60, 90, and 120 min after the
117 injections.

118

119 **2.7. RNA isolation and real-time PCR**

120 Total RNA was prepared from cells or frozen livers using RNA plus (Takara, Dalian,
121 China). The 2.5 μg total RNA was reversely transcribed with a One Step
122 PrimeScriptTM RT-PCR kit (Takara). Real-time PCR analysis was carried out using
123 the SYBR Premix-Ex Tag Kit (Takara) on an ABI prism 7500 sequence Detection
124 System (Applied Biosystems, Foster City, CA). The primer sequences are listed in
125 Table S1.

126

127 **2.8. Western blot analysis**

128 Cells and liver tissues were homogenized by using RIPA buffer (Applygen
129 Technologies Inc., Beijing, China) supplemented with protease and phosphatase
130 inhibitor (Pierce Biotechnology, Rockford, IL). Equal amount of protein was
131 subjected to 8–12% SDS-PAGE followed by transfer to PVDF membranes (Millipore,
132 Inc., Darmstadt, Germany). Membranes were blocked with 5% non-fat dry milk in
133 TBST, followed by incubation overnight with the following primary antibodies (Table
134 S2). Bolts were further incubated with HRP-conjugated secondary antibodies (Sigma)
135 and visualized with an ECL plus (Fudebio, Hangzhou, China).

136

137 **2.9. Triglyceride analysis**

138 The intrahepatic and intracellular triglyceride contents were determined by using a
139 commercial kit (Applygen Technologies Inc., Beijing, China) according the
140 manufacturer's instructions. Triglyceride values were normalized by total protein
141 contents.

142

143 **2.10. Luciferase assay**

144 To perform the luciferase reporter, plasmids containing either wild type or mutated
145 3'UTR sequence were generated (Hanyin, Shanghai, China). The plasmids were
146 transfected into HEK293T cells using Lipofectamine 3000 (Invitrogen, Carlsbad,
147 CA). The cells were also co-transfected with either the negative control or miR-376b-

148 3p mimic (100 nmol/ml). Twenty-four hours after transfection, the cells were
149 harvested according to the manufacturer's instructions (Promega Dual Luciferase
150 Assay Kit, Promega). Firefly luciferase values were normalized to those of Renilla
151 luciferase.
152
153 **2.11. Histological analysis and Oil Red O staining**
154 Livers sections were fixed in 10% neutral formalin overnight and were then
155 embedded in paraffin, after which H&E staining was performed. For Oil Red O
156 staining, 8 μm frozen liver sections were sequentially stained with Oil Red O and
157 hematoxylin (Jiancheng Biology, Nanjing, China). Cells grown in glass cover ships in
158 12-well plates were washed with PBS, and followed by staining with Oil Red O and
159 hematoxylin. Sections were imaged at 200× magnification (Olympus, Tokyo, Japan).
160
161 **2.12. Statistical analyses**
162 Statistical analyses were performed by using SPSS 18.0 for windows (SPSS, Chicago,
163 IL). Statistical comparisons were made using t-test or ANOVA where appropriate. All
164 data were expressed as mean ± standard division (SD), with a statistically significant
165 difference defined as $P < 0.05$.
166

3. Results

3.1. miR-376b-3p is downregulated in cellular and mouse models of NAFLD

By microarray analysis, we found 22 differentially expressed miRNAs, including 14 downregulated and 8 upregulated miRNAs, in HFD-fed mice compared with SCD-fed controls (Figure 1A). We performed qRT-PCR to verify the expression of downregulated miRNAs and found that miR-376b-3p was significantly down-regulated in the livers of 8-weeks HFD-fed mice compared with SCD-fed controls (Figure 1B). We observed similar result in the livers of 24-weeks WD-fed mice (Figure 1C), and in AML-12 cells and HepG2 cells stimulated by FFA for 24 h (Figure 1D and 1E). These findings indicate a potential role of miR-376b-3p in NAFLD.

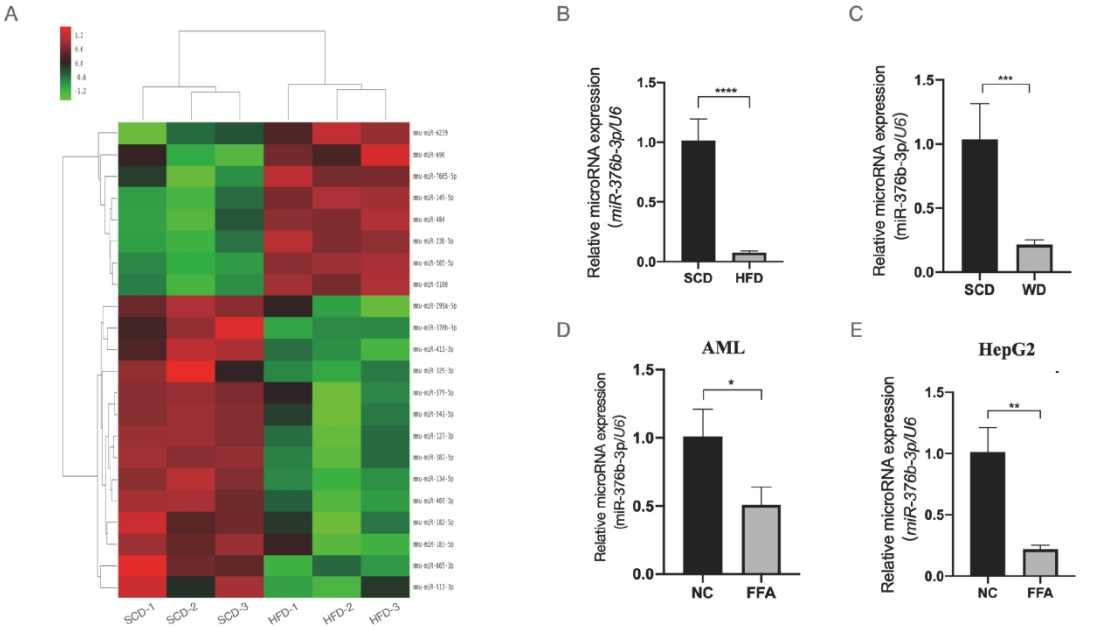

Figure 1. The differentially expressed miRNAs in livers of SCD and HFD fed mice. (A) Hierarchical clustering of the differentially expressed miRNAs in SCD and HFD fed mice. (B) Real-time PCR verification of miR-376b-3p in SCD and HFD fed mice. (C) Real-time PCR verification of miR-376b-3p in SCD and WD fed mice. (D) Real-time PCR verification of miR-376b-3p in AML-12 cells exposed to 1mM FFA. (D) Real-time PCR verification of miR-376b-3p

in HepG2 cells exposed to 1mM FFA. Data are presented as the mean ± SD of at least three independent replicates. * $P < 0.05$, ** $P < 0.01$, ***$P < 0.001$, ****$P < 0.0001$ of two-tailed student's *t*-test.

3.2. MiR-376b-3p regulates FFA-induced hepatocyte fat accumulation in vitro

To explore the function of miR-376b-3p in NAFLD, we overexpressed miR-376b-3p expression in AML-12 cells by transfection of miR-376b-3p mimic (Figure 2A). We found that overexpression of miR-376b-3p significantly decreased FFA-induced triglyceride accumulation in AML-12 cells (Figure 2B). Oil Red O staining confirmed that overexpression of miR-376b-3p significantly ameliorated FFA-induced fat accumulation in AML-12 cells (Figure 2C). In contrast, we inhibited the expression of miR-376b-3p in AML-12 cells by transfecting the cells with miR-376b-3p inhibitor (Figure 2D), and found that miR-376b-3p inhibitor significantly aggregated FFA-induced fat accumulation in AML-12 cells (Figure 2E and 2F). We observed similar results that miR-376b-3p mimic ameliorates, while miR-376b-3p inhibitor aggregates FFA-induced fat accumulation in primary hepatocytes (Figure S1A-D) and in HepG2 cells (Figure S1E-H). These findings suggested an important regulatory role of miR-376b-3p on FFA-induced fat accumulation in hepatocytes.

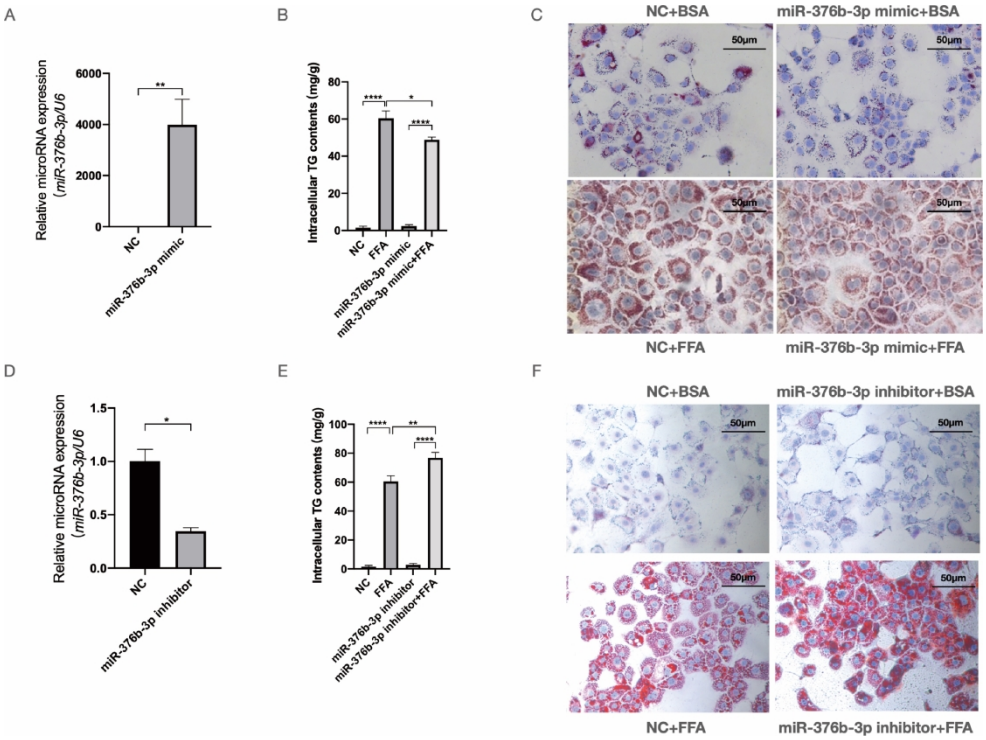

Figure 2. miR-376b-3p regulates intracellular fat accumulation in AML-12 cells.

(A) Real-time PCR confirmed miR-376b-3p mimic increased miR-376b-3p expression in AML-12 cells. (B) Overexpression of miR-376b-3p reduced the intracellular TG contents in AML-12 cells exposed to 1mM FFA for 24h. (C) Oil Red O staining conformed regulatory roles of miR-376b-3p on FFA induced hepatocytes fat accumulation (200×). (D) Real-time PCR confirmed that miR-376b-3p inhibitor decreased miR-376b-3p expression in AML-12 cells. (E) Inhibition of miR-376b-3p increased the intracellular TG contents in AML-12 cells exposed to 1mM FFA for 24h. (F) Oil Red O staining conformed aggravates roles of miR-376b-3p on FFA induced hepatocytes fat accumulation (200×). Data are presented as the mean ± SD of at least three independent replicates. * $P < 0.05$, ** $P < 0.01$, ****$P < 0.0001$ of two-tailed student's *t*-test.

3.3. MiR-376b-3p mimic ameliorates HFD-induced hepatic steatosis in mice

To further explore the regulatory role of miR-376b-3p on NAFLD in mice, we overexpressed the expression of hepatic miR-376b-3p in male C57/BL6 mice by tail vein injection of 2×10^{11} AAV8 encoding miR-376b-3p (Figure S2A and S2B), and then fed the mice with HFD or SCD for 8 weeks. We found that overexpression of hepatic miR-376b-3p significantly protected mice from HFD-induced body weight

gain (Figure 3A). The hepatic steatosis was ameliorated by miR-376b-3p overexpression as showed in gross liver (Figure 3B). Moreover, we found that overexpression of hepatic miR-376b-3p significantly decreased serum TG and TC levels in HFD-fed mice (Figure 3C), and ameliorated HFD-induced glucose and insulin intolerance, as determined by the GTT and ITT (Figure 3D and 3E). In accordance with circulating findings, mice injected with the miR-376b-3p mimic also showed lower intrahepatic TG contents (Figure 3F), and alleviated hepatic steatosis than the control mice after 8 weeks of HFD feeding (Figure 3G and 3H). These results showed that overexpression of miR-376b-3p ameliorates HFD-induced hepatic steatosis in mice.

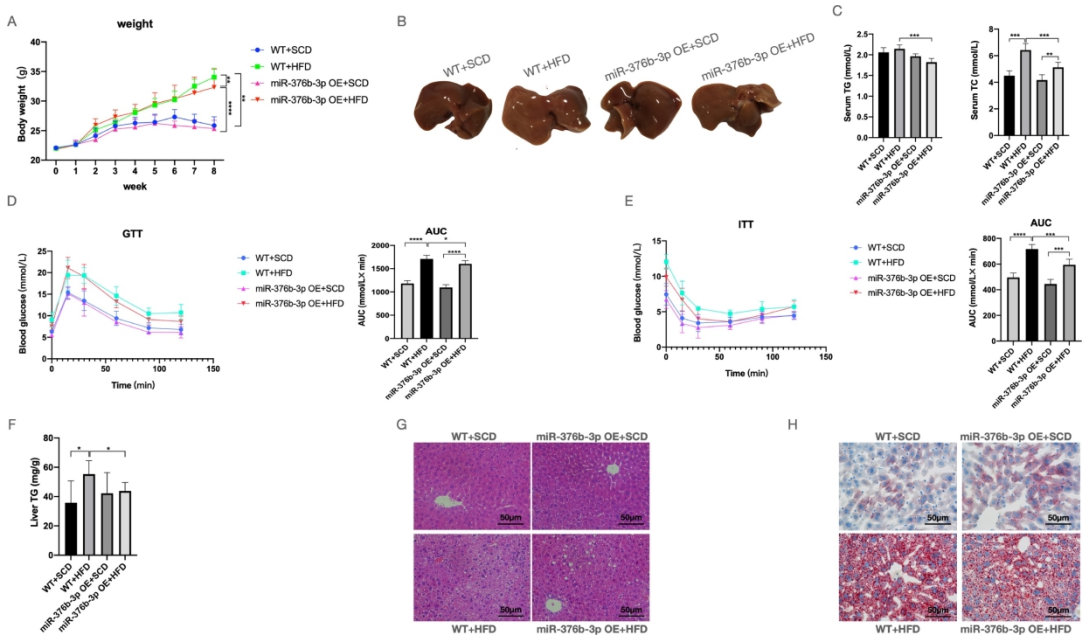

Figure 3. miR-376b-3p overexpression ameliorate HFD-induced hepatic steatosis in mice

(A) Body weights of mice. (B) Gross morphology of livers in the indicated groups. (C) Fasting blood TG (left) and TC (right) levels in mice. (D) Glucose tolerance test (GTT) with the corresponding areas under the curve (AUC) in mice. (E) Insulin tolerance test (ITT) with the corresponding AUC. (F) Liver TG contents in the indicated groups. (G) H&E staining of liver sections of the mice (200×). (H) oil-red O staining of liver sections of the mice (200×). Data are

presented as the mean ± SD of at least three independent replicates. * $P < 0.05$, ** $P < 0.01$, *** $P < 0.001$, **** $P < 0.0001$ of two-tailed student's *t*-test.

3.4. MiR-376b-3p inhibitor aggravates HFD-induced hepatic steatosis in mice

To further evaluate the effect of miR-376b-3p on HFD-induced hepatic steatosis in mice, we injected lentiviral into tail vein to inhibit hepatic miR-376b-3p in mice (Figure S2C and S2D). After 8 weeks of HFD or SCD feeding, we observed that inhibition of hepatic miR-376b-3p aggravated HFD-induced showed in body weight gain and gross liver (Figure 4A and 4B). We also found that inhibition of hepatic miR-376b-3p significantly increased serum TG and TC levels in HFD-fed mice (Figure 4C), and exacerbates HFD-induced glucose and insulin intolerance (Figure 4D and 4E). Moreover, inhibition of hepatic miR-376b-3p significantly increased intrahepatic TG level and aggregated HFD-induced hepatic steatosis in mice (Figure 4F-4H). These results showed that inhibition of miR-376b-3p exacerbates HFD-induced hepatic steatosis in mice.

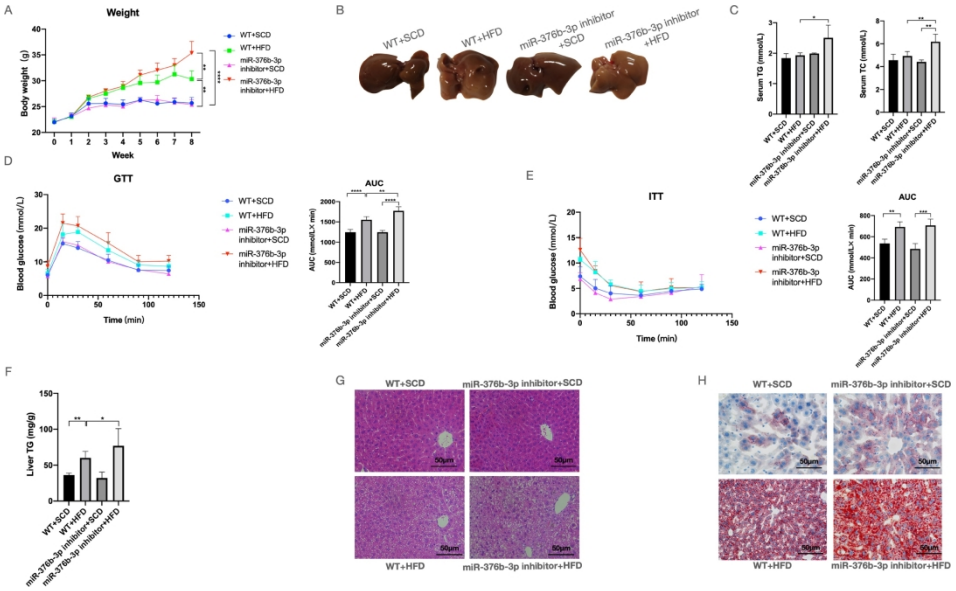

Figure 4. miR-376b-3p inhibited mice are more susceptible to HFD-induced steatosis. (A) Body weights of mice. (B) Gross morphology of livers in the indicated groups. (C) Fasting blood TG (left) and TC (right) levels in mice. (D) Glucose tolerance test (GTT) with the corresponding areas under the curve (AUC) in mice. (E) Insulin tolerance test (ITT) with the corresponding AUC. (F) Liver TG contents in the indicated groups. (G) H&E staining of liver sections of the mice (200×). (H)oil-red O staining of liver sections of the mice (200×). Data are presented as the mean ± SD of at least three independent replicates. * $P < 0.05$, ** $P < 0.01$, *** $P < 0.001$, **** $P < 0.0001$ of two-tailed student's *t*-test.

3.5. MiR-376b-3p regulates hepatic steatosis by regulating fatty acids oxidation

Lipid oxidation pathways play an important role in the pathogenesis of NAFLD. Increased expression of carnitine palmitoyltransferase 1α (CPT1α), proliferator-activated receptor-γ coactivator-1α (PGC1α), acyl-CoA oxidase1 (ACOX1) and PPARα are associated with enhanced lipid oxidation[9-11]. Therefore, we evaluated whether miR-376b-3p modulates lipid oxidation pathways both in vitro and in vivo. We found that FFA-stimulation significantly down-regulated the expression of CPT1α, PGC1α, ACOX1 and PPARα in AML-12 cells (Figure 5A and 5B). The miR-376b-3p mimic significantly up-regulated the expression of CPT1α, PGC1α, ACOX1 and PPARα, while miR-376b-3p inhibitor decreased the expression of those genes in FFA-simulated hepatocytes (Figure 5A and 5B). We observed similar moderating effects of miR-376b-3p on hepatic expression of these fatty acid oxidation genes in HFD-fed mice (Figure 5C). These findings suggested a significant regulatory role of miR-376b-3p on hepatic fatty acids oxidation, and may thereby regulate hepatic steatosis.

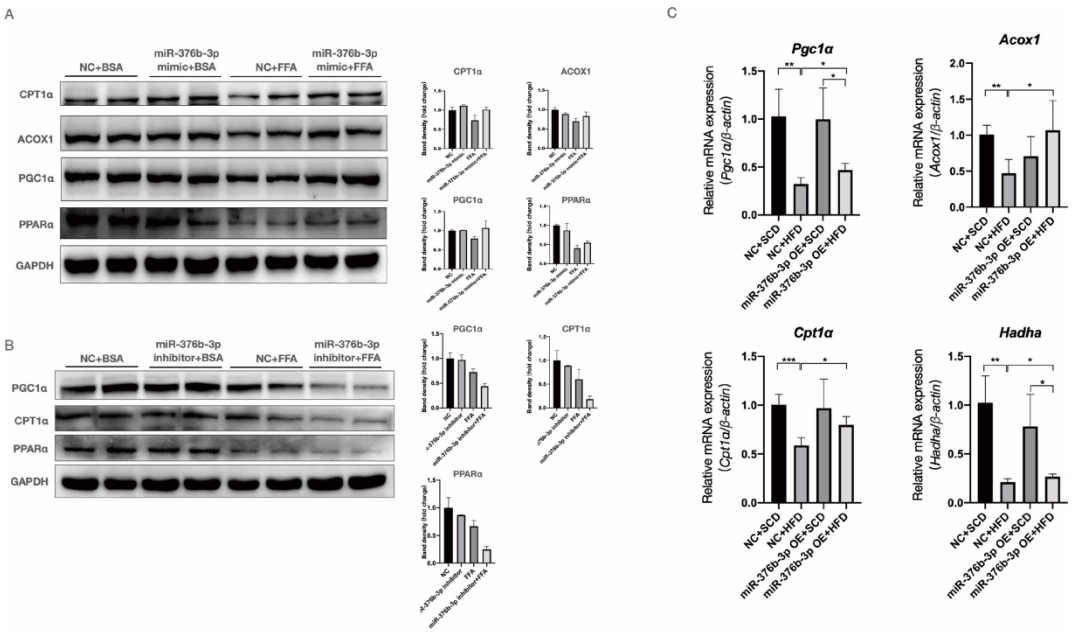

Figure 5. miR-376b-3p regulates hepatic steatosis by regulating fatty acids oxidation.
(A) Representative western-blot analyses (left) and quantification (right) of the protein levels of genes related to β-oxidation (CPT-1α, ACOX1, PGC1α and PPARα) in mouse livers. (B) Representative western-blot analyses (left) and quantification (right) of the protein levels of genes related to β-oxidation (CPT-1α, PGC1α and PPARα) in mouse livers. (C) Relative mRNA expression of genes related to β-oxidation (*Cpt1α, Acox1, Pgc1α* and *Hadha*). Data are presented as the mean ± SD of at least three independent replicates. * $P < 0.05$, ** $P < 0.01$, ***$P < 0.001$ of two-tailed student's *t*-test.

3.6. MiR-376b-3p target Fgfr1 to regulate lipid oxidation

To search for the potential target of miR-376b-3p, we used miRwalk prediction database, which predicted Fgfr1 as a miR-376b-3p target gene. FGFR1 is a well-known protein that plays a key role in lipid metabolism[12]. Based on the information above, we investigated the potential direct interaction between miR-376b-3p and Fgfr1. Bioinformatic analysis identified sequence complementarity of miR-376b-3p with the 3'UTR of Fgfr1 (Figure 6A). To verify the direct interaction between miR-

376b-3p and its putative target Fgfr1, we employed dual luciferase reporter gene assay. Delivery of miR-376b-3p suppresses Fgfr1-3'UTR luciferase activity by more than 50% (Figure 6B). Mutation of the predicted binding sites between miR-376b-3p and Fgfr1 in luciferase reporter plasmids abolished this reduction (Figure 6B). The expression of Fgfr1 increase significantly in FFA-induced AML-12 cells and HFD-fed mice, which is contrary to the expression of miR-376b-3p (Figure 6C and 6D). Furthermore, overexpression of miR-376b-3p decreased the endogenous Fgfr1 mRNA levels, while inhibition of miR-376b-3p increased the Fgfr1 expression in AML-12 cells and in the livers of mice (Figure 6E-H). These results suggested that miR-376b-3p regulates FGFR1 mRNA levels through directly binding with its 3'UTR.

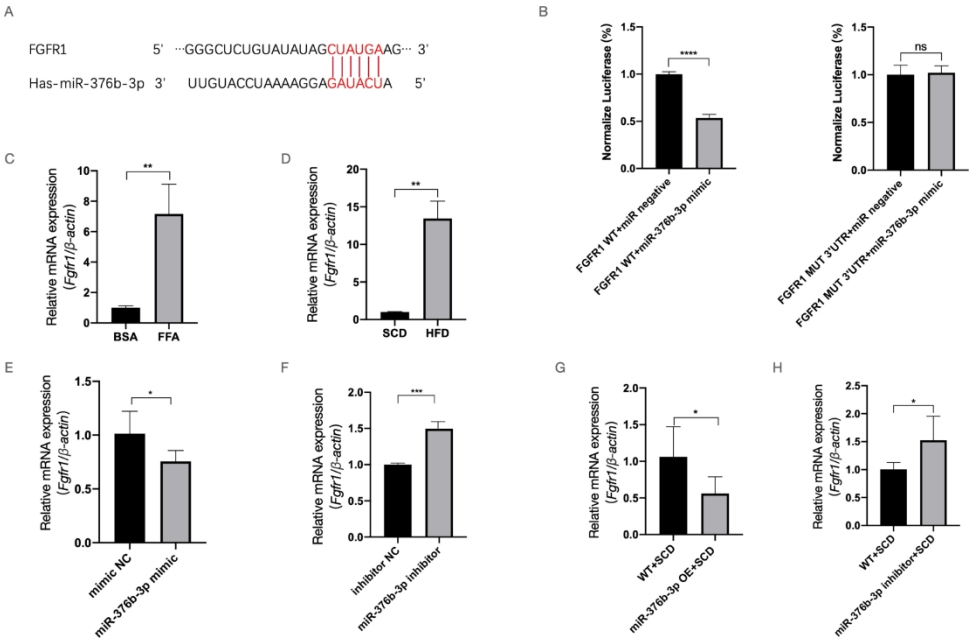

Figure 6. miR-376b-3p target 3' UTR of FGFR1.

(A) Diagram showing miR-376b-3p binding sites predicted by miRwalk in the human Fgfr1 3'UTR region. (B) Luciferase activity assays in 293T cells. (C) Relative mRNA expression of Fgfr1 in FFA treated AML-12 cells. (D) Relative mRNA expression of Fgfr1 in HFD fed mice. (E) miR-376b-3p mimic reduced the expression of Fgfr1 in AML-12 cells. (F) miR-376b-3p inhibitor increased the expression of Fgfr1 in AML-12 cells. (G) Relative mRNA expression of

Fgfr1 in miR-376b-3p overexpressed WT mice. (H) Relative mRNA expression of Fgfr1 in miR-376b-3p inhibited WT mice. * P < 0.05, ** P < 0.01, ***P < 0.001, ****P <0.0001 of two-tailed student's t-test.

Furthermore, we applied Fgfr1 siRNA and over-expression plasmids to determine the effect of Fgfr1 on fat accumulation in AML-12 cells (Figure S3A and S3B). The silence of Fgfr1 abolished the lipid deposition in FFA-stimulated miR-376b-3p inhibited AML-12 cells (Figure 7A and 7B). In contrast, overexpression of Fgfr1 significantly reversed the suppression of the lipid accumulation in FFA-stimulated miR-376b-3p overexpressed AML-12 cells (Figure 7C and 7D). Moreover, the FFA-induced β-oxidation was promoted by Fgfr1 silencing in AML-12 cells treated by miR-376b-3p inhibitor, while Fgfr1 overexpression further decreased the FFA-induced down-regulation of CPT1α and ACOX1 in miR-376b-3p mimic treated AML-12 cells (Figure 7E and 7F). These results suggested that Fgfr1 mediates the regulatory effects of miR-376b-3p on fat accumulation in hepatocytes.

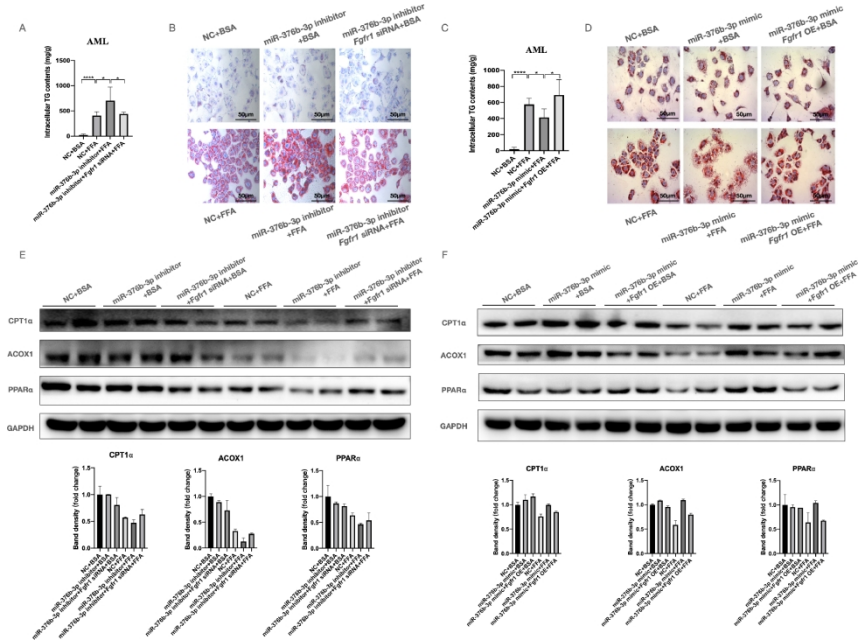

Figure 7. Fgfr1 is a target gene of miR-376b-3p involved in hepatocytes fat accumulation. (A) Intracellular TG contents in AML-12 cell. (B) Oil Red O staining in AML-12 cells (200×). (C) Intracellular TG contents in AML-12 cell. (D) Oil Red O staining in AML-12 cells (200×). (E) Protein levels of genes related to β-oxidation (CPT-1α, ACOX1and PPARα) in mouse livers. (F) Protein levels of genes related to β-oxidation (CPT-1α, ACOX1and PPARα) in mouse livers. Data are presented as the mean ± SD of at least three independent replicates. * $P < 0.05$, *** $P < 0.001$, **** $P < 0.0001$ of two-tailed student's *t*-test.

4. Discussion

In this study, we identified a role of miR-376b-3p in regulating lipid accumulation by directly targeting Fgfr1. We found that the down-regulation of miR-376b-3p in NAFLD models and confirmed the importance of miR-376b-3p for liver function by loss- or gain-of-function experiment. Additionally, we uncovered a significant role for miR-376b-3p in regulation of hepatic lipid oxidation, and identified that Fgfr1 is a downstream target of miR-376b-3p. This newly miR-376b-3p-Fgfr1 pathway provides a novel clue to the pathogenesis of lipid deposition in NAFLD. MiR-376b-3p may become a potential target for NAFLD treatment.

Growing evidence demonstrated that miRNAs are crucial regulators in metabolic diseases including NAFLD, such as miR-378, miR-122, miR-149-5p, and miR-34a[8, 13-15]. The function of miR-376b-3p has been well studied in several diseases[16-18]. For example, it has been reported that miR-376b-3p expressed at high levels in pancreatic islets and relates to type-2 diabetes[17, 19, 20]. But the role of miR-376b-3p in NAFLD has never been studied. Our microarray analysis found that multiple

351 miRNAs, including miR-376b-3p, have significant reduction in HFD-fed mice
352 compared with SCD-fed mice. Although the change in microarray results is not the
353 most obvious, it is verified to be down-regulated the most stable and significant in
354 multiple animal and cell models. Microarray analysis in previous studies also
355 implying a potential role of miR-376b-3p in metabolism-related diseases. For
356 instance, data in chip GSE65978 shows that the expression of miR-376b-3p in mice
357 fed on a high-fat diet without exercise is significantly reduce compared to those
358 exercised mice fed high-fat diet. Db/db induced diabetes mice model significantly
359 down-regulated the expression of miR-376b-3p in liver (GSE17035) and skeletal
360 muscle (GSE32376) than normal control mice. Apart from this, the expression of
361 some other miRNAs in the same cluster, such as miR-376a-3p, miR-376c-3p, and
362 miR-382-5p, is also declined significantly after HFD treatment (results are not shown
363 here). It is suggested that the cluster where miR-376b-3p is located may have a
364 specific role in NAFLD. The synergy of these miRNAs in the cluster in NAFLD will
365 be further explored in our future studies.
366
367 We further confirmed the moderating effect of miR-376b-3p in NAFLD and explored
368 its downstream mechanisms. The accumulation of hepatic lipids results from the
369 imbalance between lipid acquisition and lipid disposal. Oxidation of fatty acids is one
370 of the two major pathways of lipid disposal, which is controlled by PPARα and
371 occurs mainly in the mitochondria[21, 22]. The entry of fatty acids into the
372 mitochondria depends on CPT1α, whereas ACOX1 substrates as an endogenous

activator of PPARα[23, 24]. In addition, PGC-1α controls oxidative metabolism by regulating both the biogenesis and the intrinsic properties of the mitochondria[23]. Thence, we detected the expression of these key factors in lipid oxidation pathway when miR-376b-3p was intervened. Our results showed that overexpression of miR-376b-3p ameliorated FFA-induced hepatocytes lipid accumulation and promoted fatty acids oxidation. Otherwise, inhibition of miR-376b-3p had the opposite effects. Therefore, our results provide evidences for the first time that miR-376b-3p regulates lipid deposition through fatty acid oxidation pathways.

MicroRNAs regulate the expression and translation of target mRNAs at the post-transcriptional level by binding to their 3' UTR. Bioinformatic analysis was used to predict target genes, and we identified that Fgfr1 may have interaction with miR-376b-3p. FGFR1 is a receptor of metabolic regulation proteins FGF21[25], which is believed to be a predictor and therapeutic target for NAFLD[26, 27]. Studies have reported that Fgfr1 is related to brown fat stimulation, insulin sensitization, lipid metabolism in type 2 diabetes or obesity patients, which are closely interrelated to NAFLD[28]. We used the dual luciferase reporter gene experiment to prove that miR-376b-3p and Fgfr1 do have a direct interaction. The effect of intervened Fgfr1 on the regulation of lipid transformation caused by miR-376b-3p further confirmed that miR-376b-3p can mediate the lipid accumulation process through Fgfr1.

In our study, we reveal that miR-376b-3p regulates hepatic lipid accumulation targeting Fgfr1 in NAFLD progress, and miR-376b-3p may be a potential therapeutic target. However, there are still several limitations in this study. First, the regulation and function of miRNAs are very complicated, Fgfr1 may not be the only main target. Further investigations of miR-376b-3p regulation mechanism are needed to clarify. Second, although we found that miRNAs in the same cluster of miR-376b-3p may also have regulatory effects in NAFLD, we have not conducted depth exploration in this study, which will be continue to investigated in later studies. In addition, even though the results in animals and cells have clearly demonstrated the regulatory effects and potential mechanisms of miR-376b-3p in NAFLD, its clinical verification and application are still challenging.

In conclusion, our study demonstrated that miR-376b-3p was downregulated in NAFLD and has a novel regulatory role in lipid oxidation through miR-376b-3p-Fgfr1 dependent mechanism.

5. Conclusions

MiR-376b-3p was downregulated in NAFLD and has a novel regulatory role in lipid oxidation through miR-376b-3p-Fgfr1 dependent mechanism.

Acknowledgments

This study is supported by National Natural Science Foundation of China (81770573, 81870400, 82070585).

Conflicts of Interest

The authors declare no conflict of interest associated with this manuscript.

Authors' Contributions

Xin-Yu Wang designed and supervised the study; Lin-Jie Lu, You-Ming Li conducted experiments or interpreted the data; Cheng-Fu Xu wrote the manuscript.

Supplementary Materials

Supplementary data containing primer sequences, additional qPCR figures and oil red O staining images. Table S1: Primer sequences of genes analyzed by Real-time PCR. Table S2: Protein antibodies for Western blot analysis. Figure S1. miR-376b-3p regulates intracellular fat accumulation in primary hepatocytes and HepG2 cells. Figure S2. miR-376b-3p was overexpressed or inhibited in mice liver. Figure S3. The expression of Fgfr1 was changed by transfection of siRNA or overexpression plasmids.

References

[1] Guidelines of prevention and treatment for nonalcoholic fatty liver disease: a 2018 update. *Zhonghua Gan Zang Bing Za Zhi*. **26**: 195-203 (2018).

[2] Rinella ME. Nonalcoholic fatty liver disease: a systematic review. *Jama*. **313**: 2263-73 (2015).

[3] Zhou F, Zhou J, Wang W, Zhang XJ, Ji YX, Zhang P*, et al.* Unexpected Rapid Increase in the Burden of NAFLD in China From 2008 to 2018: A Systematic Review and Meta-Analysis. *Hepatology*. **70**: 1119-33 (2019).

[4] Adams LA, Anstee QM, Tilg H, Targher G. Non-alcoholic fatty liver disease and its relationship with cardiovascular disease and other extrahepatic diseases. *Gut*. **66**: 1138-53 (2017).

[5] Dong H, Lei J, Ding L, Wen Y, Ju H, Zhang X. MicroRNA: function, detection, and bioanalysis. *Chem Rev*. **113**: 6207-33 (2013).

[6] Cheung O, Puri P, Eicken C, Contos MJ, Mirshahi F, Maher JW*, et al.* Nonalcoholic steatohepatitis is associated with altered hepatic MicroRNA expression. *Hepatology*. **48**: 1810-20 (2008).

[7] Wu GY, Rui C, Chen JQ, Sho E, Zhan SS, Yuan XW*, et al.* MicroRNA-122 Inhibits Lipid Droplet Formation and Hepatic Triglyceride Accumulation via Yin Yang 1. *Cell Physiol Biochem*. **44**: 1651-64 (2017).

[8] Ding J, Li M, Wan X, Jin X, Chen S, Yu C*, et al.* Effect of miR-34a in regulating steatosis by targeting PPARα expression in nonalcoholic fatty liver disease. *Sci Rep*. **5**: 13729 (2015).

455 [9] Nguyen TTT, Shang E, Shu C, Kim S, Mela A, Humala N*, et al.* Aurora kinase A
456 inhibition reverses the Warburg effect and elicits unique metabolic vulnerabilities in
457 glioblastoma. *Nat Commun*. **12**: 5203 (2021).
458 [10] Yu Q, Chen X, Sun X, Li W, Liu T, Zhang X*, et al.* Pectic Oligogalacturonide
459 Facilitates the Synthesis and Activation of Adiponectin to Improve Hepatic Lipid
460 Oxidation. *Mol Nutr Food Res*. e2100167 (2021).
461 [11] Tahri-Joutey M, Andreoletti P, Surapureddi S, Nasser B, Cherkaoui-Malki M,
462 Latruffe NJIjoms. Mechanisms Mediating the Regulation of Peroxisomal Fatty Acid
463 Beta-Oxidation by PPARα. **22**: (2021).
464 [12] Park S, Choi Y, Um SJ, Yoon SK, Park T. Oleuropein attenuates hepatic steatosis
465 induced by high-fat diet in mice. *J Hepatol*. **54**: 984-93 (2011).
466 [13] Zhang T, Duan J, Zhang L, Li Z, Steer CJ, Yan G*, et al.* LXRα Promotes
467 Hepatosteatosis in Part Through Activation of MicroRNA-378 Transcription and
468 Inhibition of Ppargc1β Expression. *Hepatology*. **69**: 1488-503 (2019).
469 [14] Tsai WC, Hsu SD, Hsu CS, Lai TC, Chen SJ, Shen R*, et al.* MicroRNA-122
470 plays a critical role in liver homeostasis and hepatocarcinogenesis. *J Clin Invest*. **122**:
471 2884-97 (2012).
472 [15] Chen S, Chen D, Yang H, Wang X, Wang J, Xu C. Uric acid induced hepatocytes
473 lipid accumulation through regulation of miR-149-5p/FGF21 axis. *BMC*
474 *Gastroenterol*. **20**: 39 (2020).

475 [16] Wu X, Li J, Ren Y, Zuo Z, Ni S, Cai J. MEG3 can affect the proliferation and
476 migration of colorectal cancer cells through regulating miR-376/PRKD1 axis. *Am J*
477 *Transl Res*. **11**: 5740-51 (2019).
478 [17] Chakraborty C, Doss CG, Bandyopadhyay S, Agoramoorthy G. Influence of
479 miRNA in insulin signaling pathway and insulin resistance: micro-molecules with a
480 major role in type-2 diabetes. *Wiley Interdiscip Rev RNA*. **5**: 697-712 (2014).
481 [18] An N, Luo X, Zhang M, Yu R. MicroRNA-376b promotes breast cancer
482 metastasis by targeting Hoxd10 directly. *Exp Ther Med*. **13**: 79-84 (2017).
483 [19] Poy MN, Eliasson L, Krutzfeldt J, Kuwajima S, Ma X, Macdonald PE*, et al.* A
484 pancreatic islet-specific microRNA regulates insulin secretion. *Nature*. **432**: 226-30
485 (2004).
486 [20] Joglekar MV, Joglekar VM, Hardikar AA. Expression of islet-specific
487 microRNAs during human pancreatic development. *Gene Expr Patterns*. **9**: 109-13
488 (2009).
489 [21] Ipsen DH, Lykkesfeldt J, Tveden-Nyborg P. Molecular mechanisms of hepatic
490 lipid accumulation in non-alcoholic fatty liver disease. *Cell Mol Life Sci*. **75**: 3313-27
491 (2018).
492 [22] Reddy JK, Hashimoto T. Peroxisomal beta-oxidation and peroxisome
493 proliferator-activated receptor alpha: an adaptive metabolic system. *Annu Rev Nutr*.
494 **21**: 193-230 (2001).
495 [23] Nassir F, Ibdah JA. Role of mitochondria in nonalcoholic fatty liver disease. *Int J*
496 *Mol Sci*. **15**: 8713-42 (2014).

[24] Fan CY, Pan J, Usuda N, Yeldandi AV, Rao MS, Reddy JK. Steatohepatitis, spontaneous peroxisome proliferation and liver tumors in mice lacking peroxisomal fatty acyl-CoA oxidase. Implications for peroxisome proliferator-activated receptor alpha natural ligand metabolism. *J Biol Chem*. **273**: 15639-45 (1998).

[25] Sonoda J, Chen M, Baruch AJHmb, investigation c. FGF21-receptor agonists: an emerging therapeutic class for obesity-related diseases. **30**: (2017).

[26] Tillman E, Rolph TJFie. FGF21: An Emerging Therapeutic Target for Non-Alcoholic Steatohepatitis and Related Metabolic Diseases. **11**: 601290 (2020).

[27] Li H, Dong K, Fang Q, Hou X, Zhou M, Bao Y*, et al.* High serum level of fibroblast growth factor 21 is an independent predictor of non-alcoholic fatty liver disease: a 3-year prospective study in China. *J Hepatol*. **58**: 557-63 (2013).

[28] Kolumam G, Chen MZ, Tong R, Zavala-Solorio J, Kates L, van Bruggen N*, et al.* Sustained Brown Fat Stimulation and Insulin Sensitization by a Humanized Bispecific Antibody Agonist for Fibroblast Growth Factor Receptor 1/βKlotho Complex. *EBioMedicine*. **2**: 730-43 (2015).